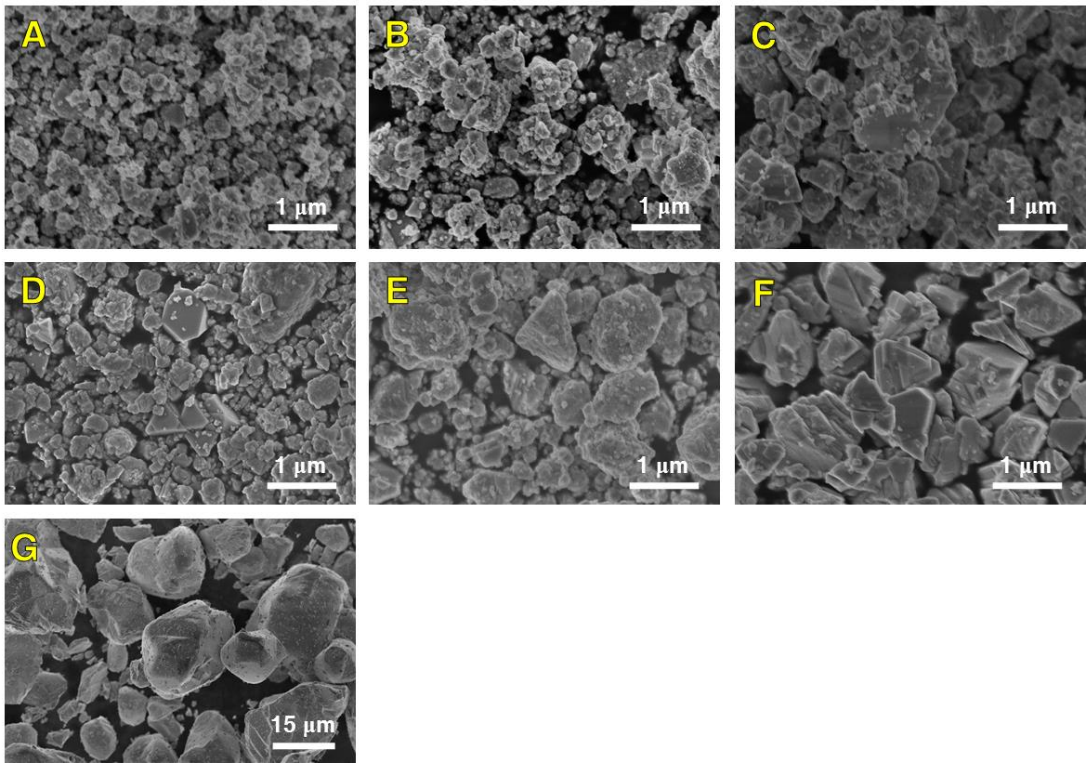

Fig. S1. SEM images of series $(ZnSe)_x(CuGa_{2.5}Se_{4.25})_{1-x}$ selenides with different molar ratios of Zn/(Zn+Cu): (A) x = 0, (B) 1/6, (C) 1/3, (D) 1/2, (E) 2/3, (F) 5/6, and (G) 1.

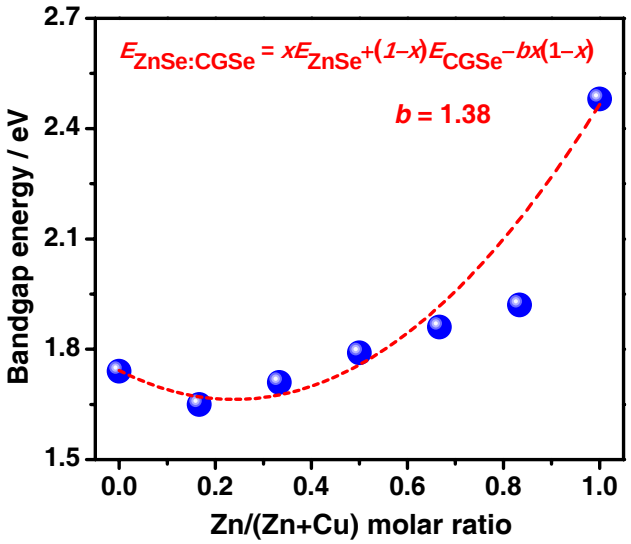

Fig. S2. Bandgap energy as a function of the Zn/(Zn+Cu) molar ratio for $(ZnSe)_x(CuGa_{2.5}Se_{4.25})_{1-x}$ samples.

As shown in this Figure, the bandgap energy exhibited a nonlinear dependence on the Zn/(Zn+Cu) ratio of the solid solutions. By fitting the data based on the equation shown above, the equation of the fitted curve is $y = 1.74 - 0.66x + 1.38x^2$. According to this fitted equation, it is estimated that the bowing parameter of b is 1.38, and the lowest bandgap energy is at a composition of $x = 0.24$.

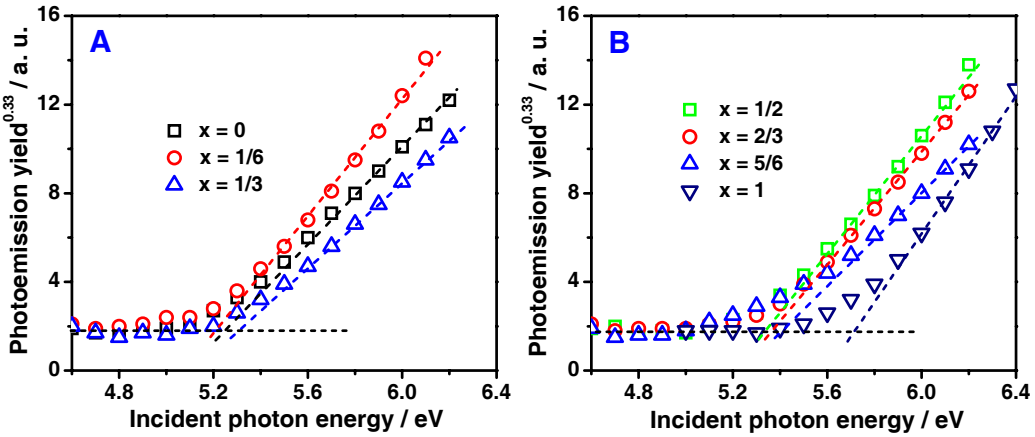

Fig. S3. PESA of bare $(ZnSe)_x(CuGa_{2.5}Se_{4.25})_{1-x}$ photoelectrodes with different molar ratios of Zn/(Zn+Cu): (A) $x = 0$; $x = 1/6$ and $x = 1/3$, (B) $x = 1/2$; $x = 2/3$; $x = 5/6$ and $x = 1$.

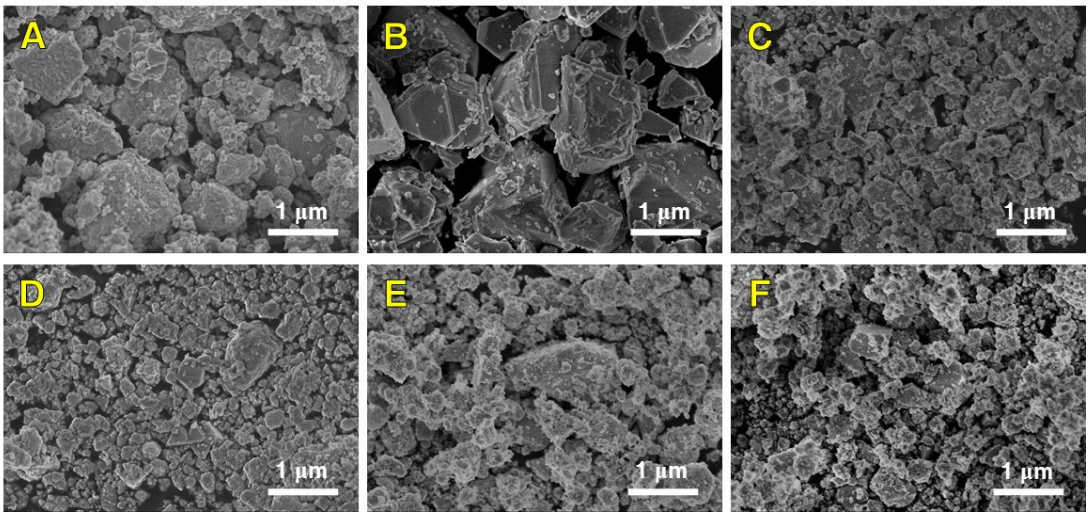

Fig. S4. SEM images of series $(ZnSe)_{0.5}(CGSe)_{0.5}$ selenides with different molar ratios of Ga/Cu: (A) Ga/Cu = 1.0, (B) 1.5, (C) 2.0, (D) 2.5, (E) 3.0, and (F) 3.5.

Indefinite morphologies, coarse surfaces, and wide distributions in sizes ranging from hundreds of nanometers to several micrometers was confirmed from those images. Here, the cases of Ga/Cu = 1.0 and 1.5 showed slightly larger particle sizes compared with the other cases. This result is similar to our previous work (H. Kumagai, T. Minegishi, Y. Moriya, J. Kubota and K. Domen, *J. Phys. Chem. C*, 2014, **118**, 16386–16392) on the CGSe system, in which CGSe particles showed relatively large sizes when the Ga/Cu molar ratio was at around 1.

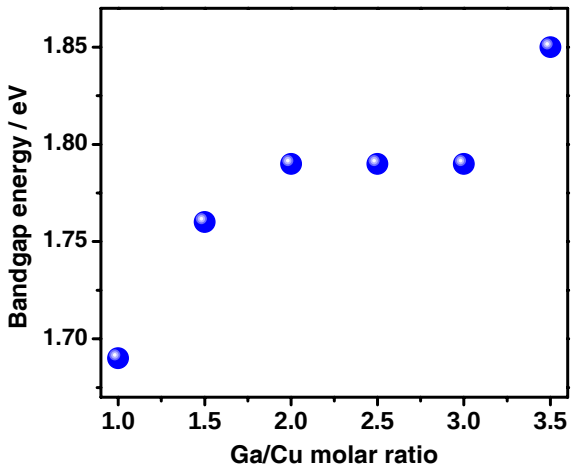

Fig. S5. Bandgap energy as a function of the Ga/Cu molar ratio for $(ZnSe)_{0.5}(CGSe)_{0.5}$ samples.

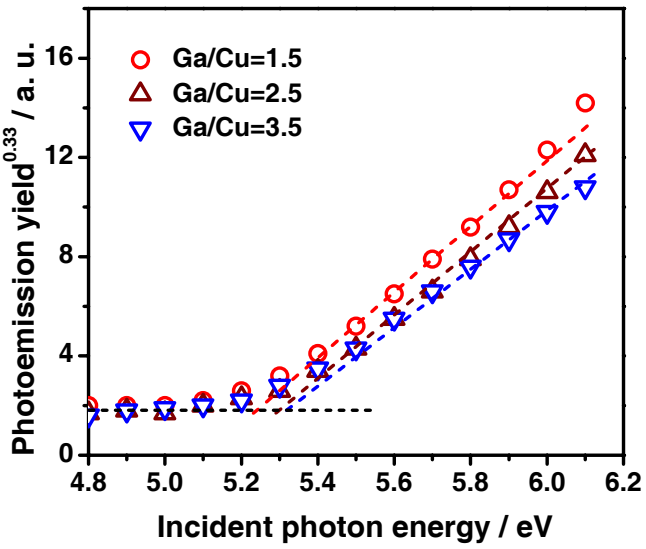

Fig. S6. PESA of bare $(ZnSe)_{0.5}(CGSe)_{0.5}$ photoelectrodes with different molar ratios of Ga/Cu.

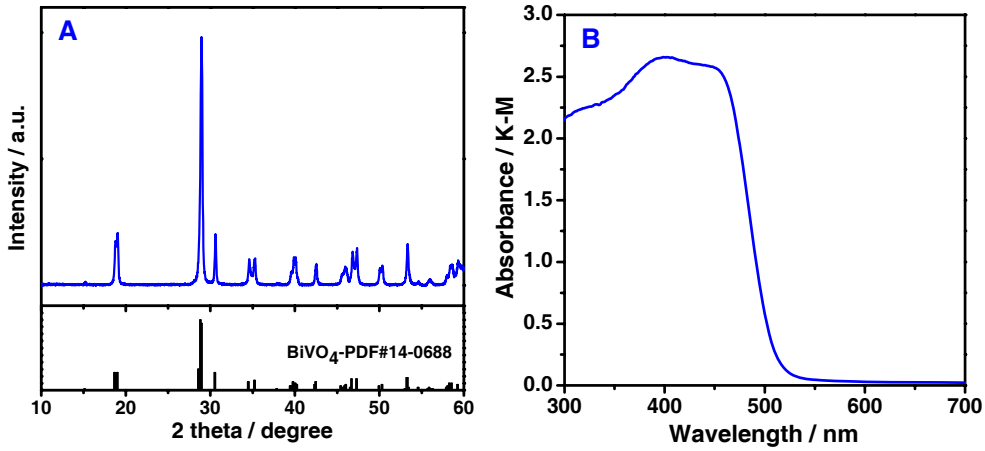

Fig. S7. XRD pattern (A) and UV-vis DRS (B) of the prepared $BiVO_4$ sample.

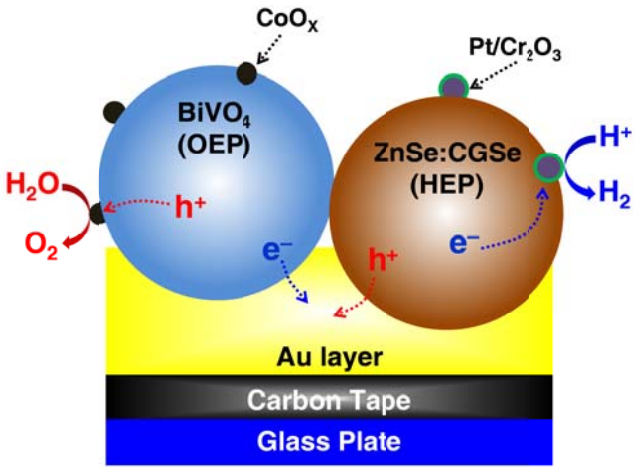

Fig. S8. Schematic image of the prepared ZnSe:CGSe/Au/$BiVO_4$ sheet system for Z-scheme pure-water splitting.

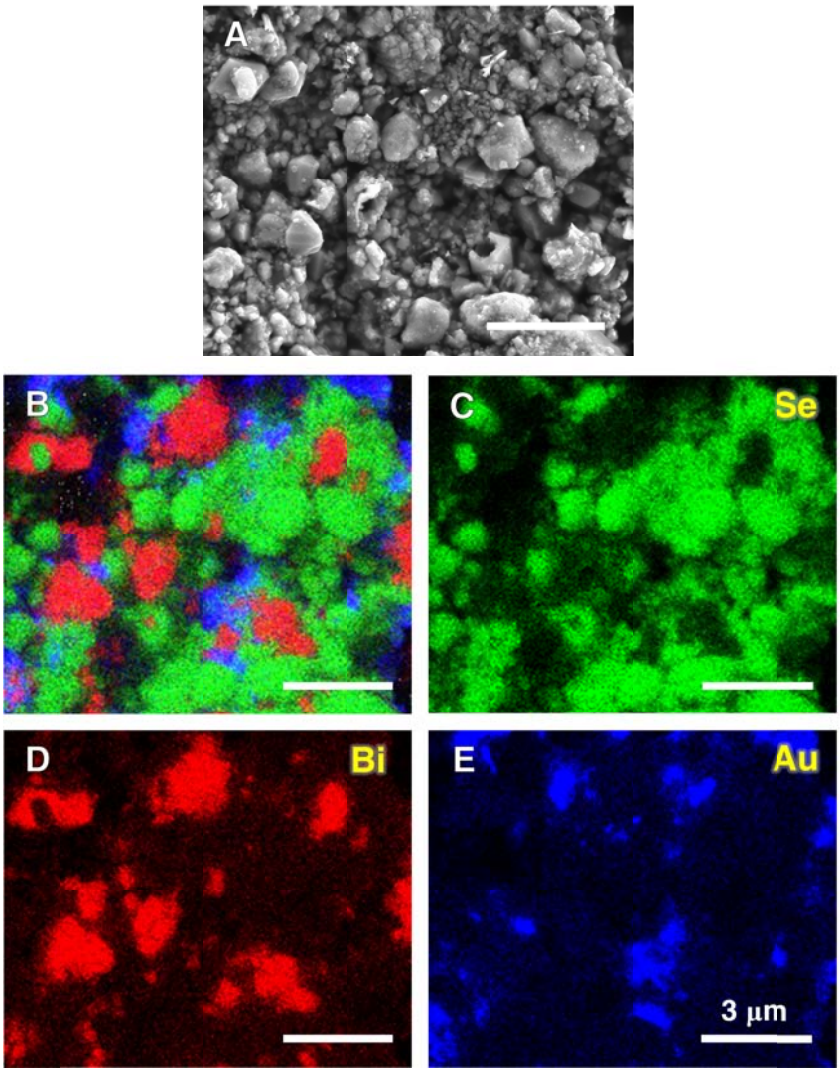

Fig. S9. Top-view SEM image and SEM-EDS mapping images of $(ZnSe)_{0.5}(CuGa_{2.5}Se_{4.25})_{0.5}$/Au/$BiVO_4$ sheet sample.

(A) Typical top-view SEM image of $(ZnSe)_{0.5}(CuGa_{2.5}Se_{4.25})_{0.5}$/Au/$BiVO_4$ sheet.

(B−E) SEM-EDS mapping images showing (B) a superimposition of all elements, (C) Se, (D) Bi and (E) Au.

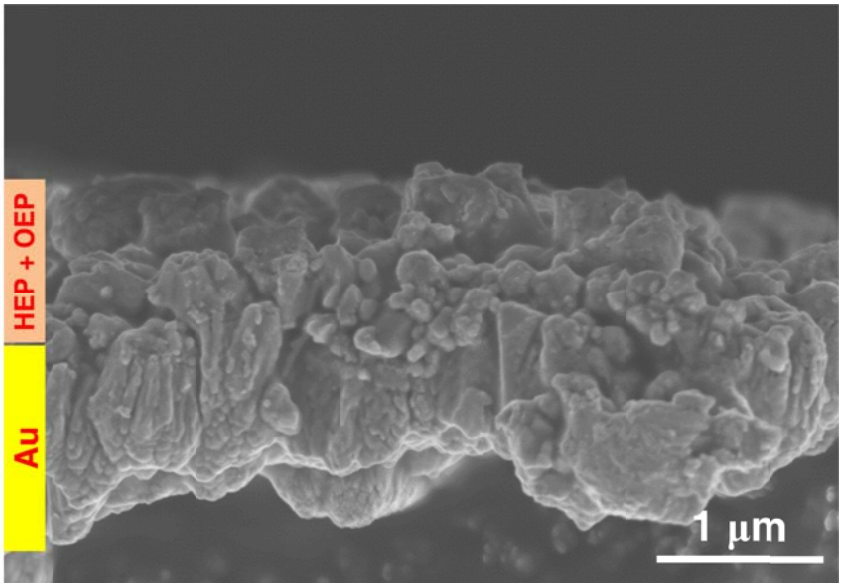

Fig. S10. Typical cross-sectional SEM image of the $(ZnSe)_{0.5}(CuGa_{2.5}Se_{4.25})_{0.5}$/Au/$BiVO_4$ sheet sample. HEP and OEP stand for hydrogen evolution photocatalyst and oxygen evolution photocatalyst, respectively.

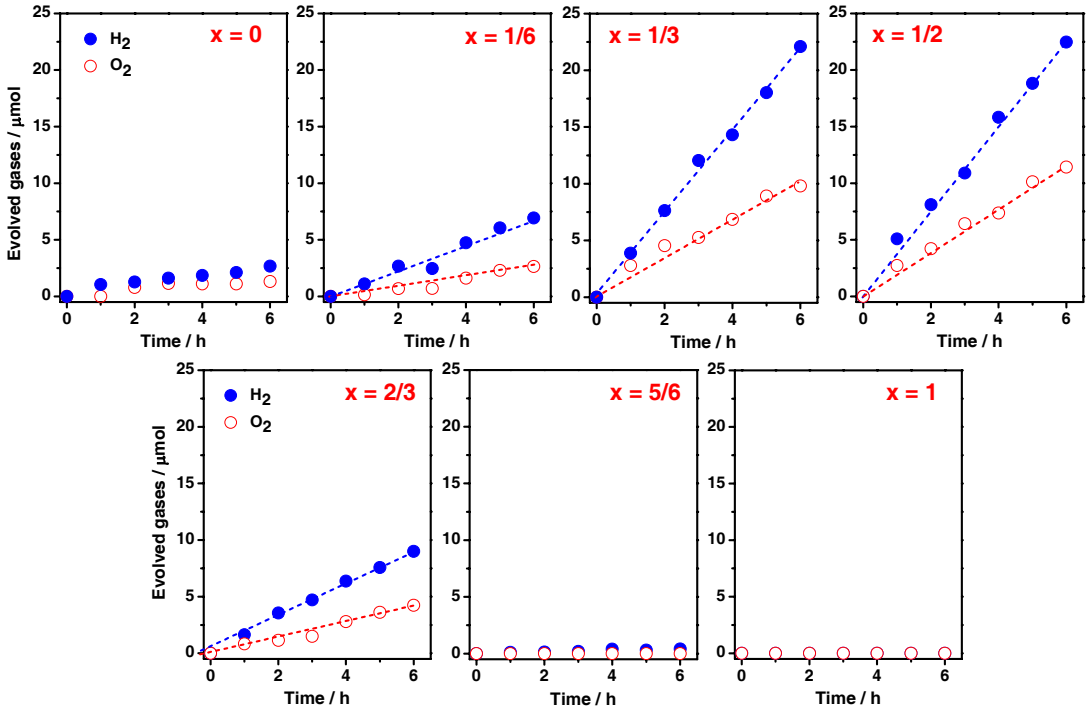

Fig. S11. Time courses of overall water splitting over $(ZnSe)_x(CuGa_{2.5}Se_{4.25})_{1-x}$/Au/$BiVO_4$ sheets with different molar ratios of Zn/(Zn+Cu). Reaction conditions: distilled water (40 mL); light source: 300 W xenon lamp equipped with a visible light filter (λ > 420 nm); irradiation area: 9 cm^2; reduction cocatalyst: 0.16 μmol Pt, Pt/Cr = 2; oxidation cocatalyst: 0.5 wt% CoO_x (with respect to $BiVO_4$).

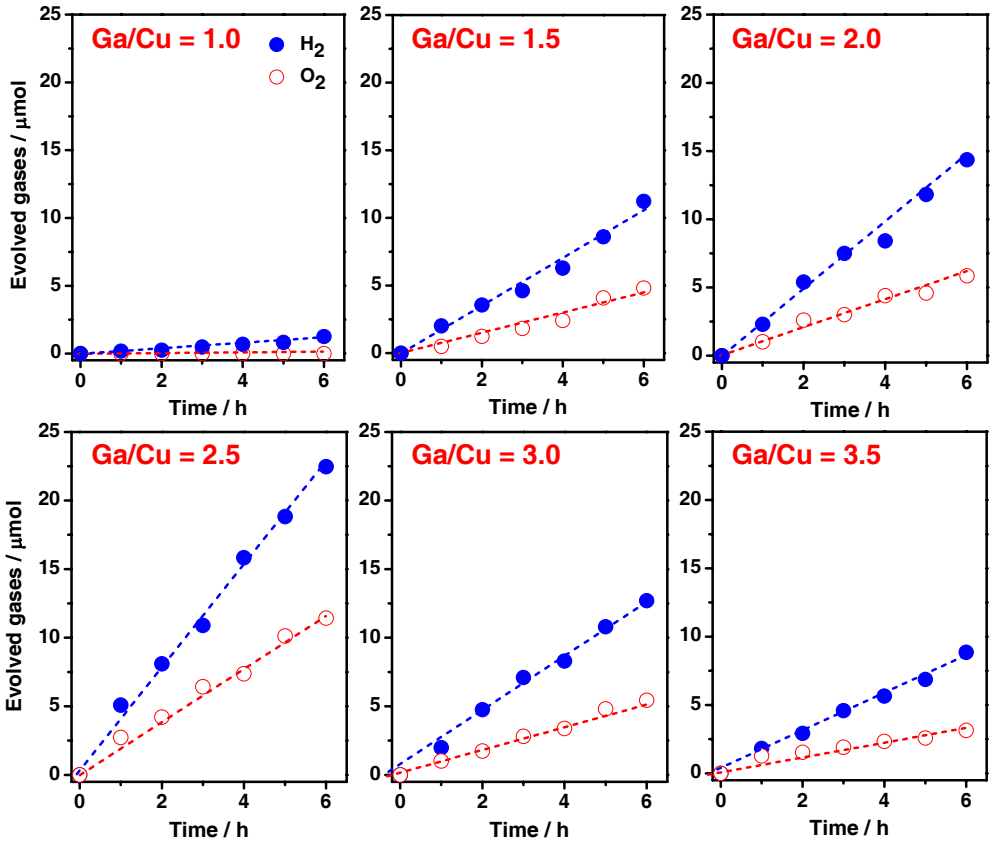

Fig. S12. Time courses of overall water splitting over $(ZnSe)_{0.5}(CGSe)_{0.5}$/Au/$BiVO_4$ sheets with different molar ratios of Ga/Cu. Reaction conditions: distilled water (40 mL); light source: 300 W xenon lamp equipped with a visible light filter ($\lambda > 420$ nm); irradiation area: 9 cm^2; reduction cocatalyst: 0.16 μmol Pt, Pt/Cr = 2; oxidation cocatalyst: 0.5 wt% CoO_x (with respect to $BiVO_4$).

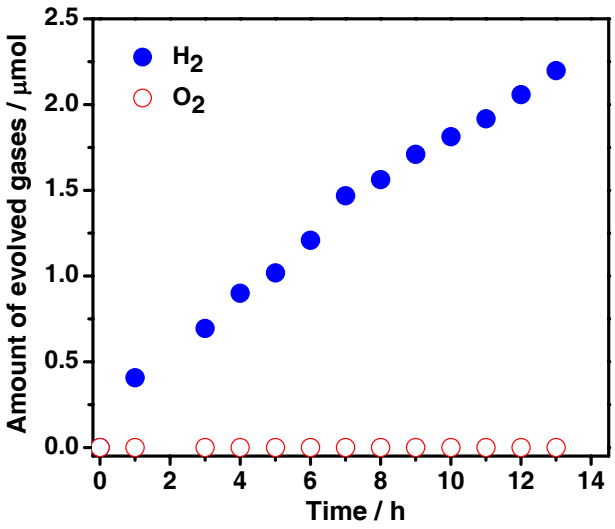

Fig. S13. Time courses of water splitting over $(ZnSe)_{0.5}(CuGa_{2.5}Se_{4.25})_{0.5}/BiVO_4$ sheet without a Au layer. Reaction conditions: distilled water (40 mL); light source: 300 W xenon lamp equipped with a visible light filter (λ > 420 nm); irradiation area: 9 cm^2; reduction cocatalyst: 0.16 μmol Pt, Pt/Cr = 2; oxidation cocatalyst: 0.5 wt% CoO_x (with respect to $BiVO_4$).

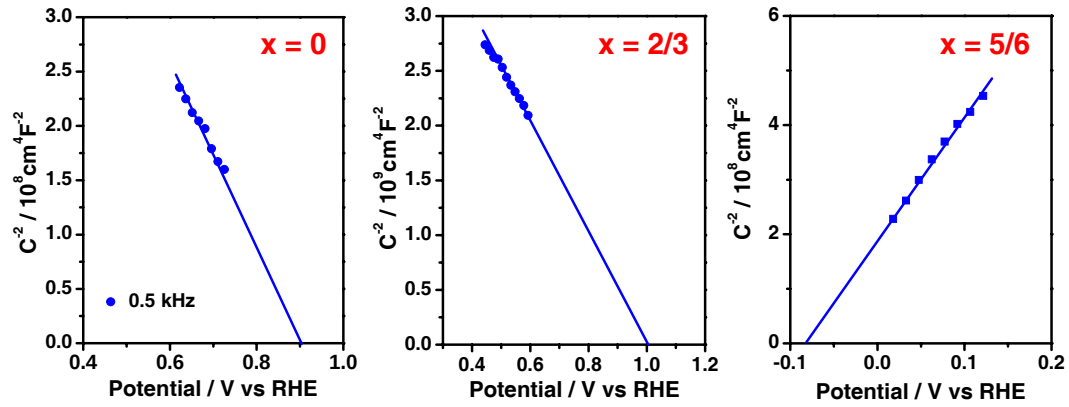

Fig. S14. Mott-Schottky plots of bare $(ZnSe)_x(CuGa_{2.5}Se_{4.25})_{1-x}$ photoelectrodes with different molar ratios of Zn/(Zn+Cu) at frequency of 0.5 kHz.